

Supporting information

The role of halogens in on-surface Ullmann polymerization

Gianluca Galeotti,¹ Marco Di Giovannantonio,^{2,§} Josh Lipton-Duffin,³ Maryam Ebrahimi,^{1,} Stefano Tebi,² Alberto Verdini,⁴ Luca Floreano,⁴ Yannick Fagot-Revurat,⁵ Dmitrii F. Perepichka,⁶ Federico Rosei,^{1,*} Giorgio Contini,^{2,7,*}*

¹ Centre Énergie, Matériaux et Télécommunications, Institut National de la Recherche Scientifique, 1650 Boulevard Lionel-Boulet, Varennes, QC, J3X 1S2, Canada

² Istituto di Struttura della Materia, CNR, Via Fosso del Cavaliere 100, 00133 Roma, Italy

³ School of Chemistry, Physics and Mechanical Engineering, and Institute for Future Environments, Queensland University of Technology (QUT), 2 George Street, Brisbane, QLD 4001, Australia

⁴ CNR-IOM, Laboratorio TASC, 34149 Trieste, Italy

⁵ Institut Jean Lamour, UMR 7198, Université Lorraine/CNRS, B.P. 239 FE-54506, Vandoeuvre-les-Nancy, France

⁶ Department of Chemistry, McGill University, 801 Sherbrooke Str. West, Montreal, QC H3A 2K6, Canada

⁷ Department of Physics, University of Rome Tor Vergata, Via della Ricerca Scientifica 1, 00133 Roma, Italy

[§] Present address: Empa - Swiss Federal Laboratories for Materials Science and Technology, Überlandstrasse 129, 8600 Dübendorf, Switzerland.

* Corresponding authors e-mails: giorgio.contini@cnr.it, rosei@emt.inrs.ca, maryam.ebrahimi@emt.inrs.ca

1. Polymerization temperature

Table S 1. T_{start} and T_{end} of the polymerization reaction, obtained from fast-XPS map in Figure 1, at the temperatures at which 10% and 90% of the reaction is completed, respectively and the temperature range of polymerization (ΔT , measured as $T_{\text{end}} - T_{\text{start}}$).

| Molecule | $T_{\text{start}}(^{\circ}\text{C})$ | $T_{\text{end}}(^{\circ}\text{C})$ | $\Delta T(^{\circ}\text{C})$ |
|----------|--------------------------------------|------------------------------------|------------------------------|
| dIB | 126 | 208 | 82 |
| BIB | 123 | 166 | 43 |
| dBB | 175 | 209 | 34 |
| BCB | 174 | 210 | 36 |
| dCB | 185 | 220 | 35 |

2. dIB vs other precursors

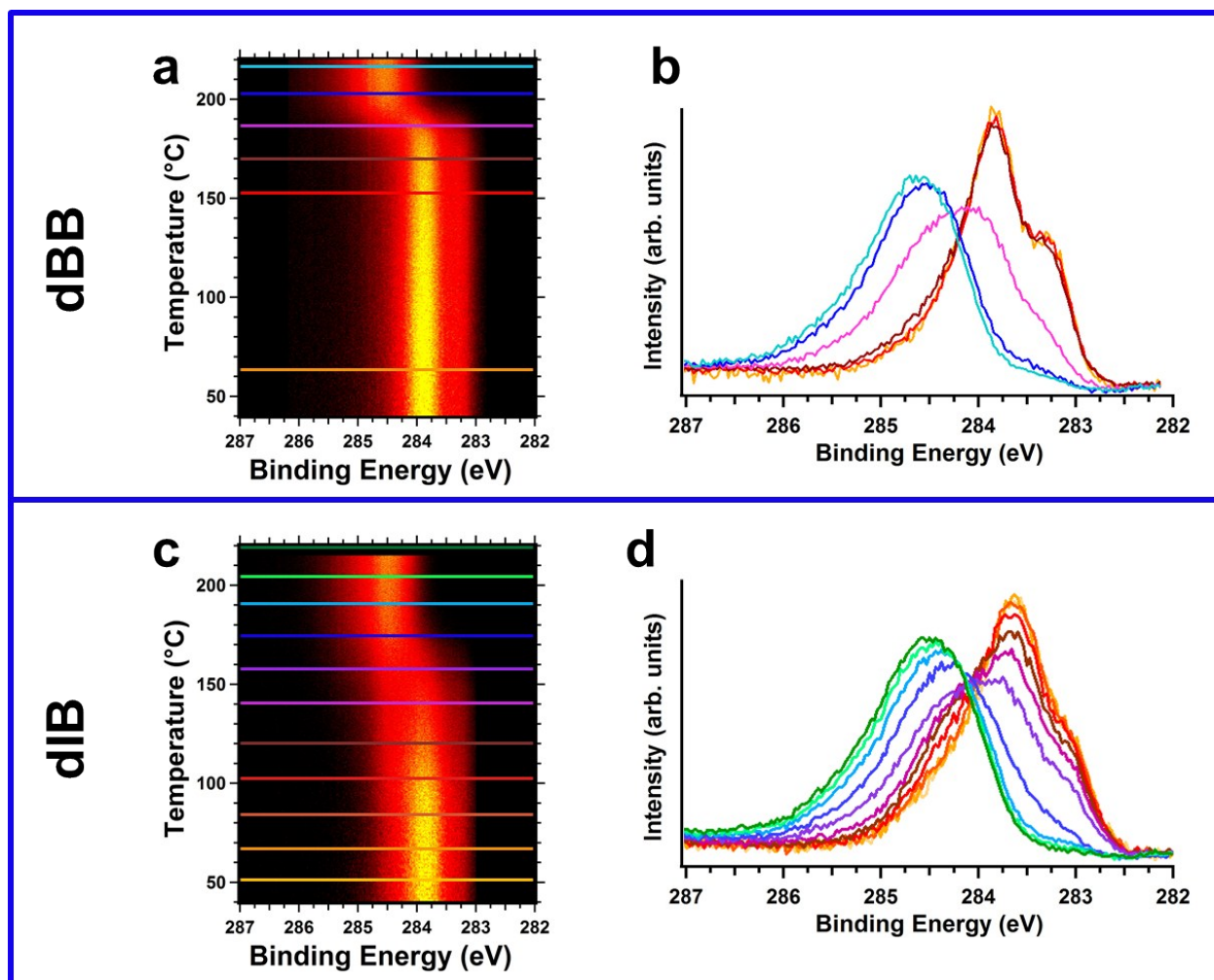


Figure S 1. Fast-XPS measurements of C 1s core level during annealing of a saturated coverage of dBB (a) and dIB (c) on Cu(110). C 1s spectra from map at 20 °C interval are reported in the panels b and d.

3. Cu(110) directions and $c(2 \times 2)$ superstructure

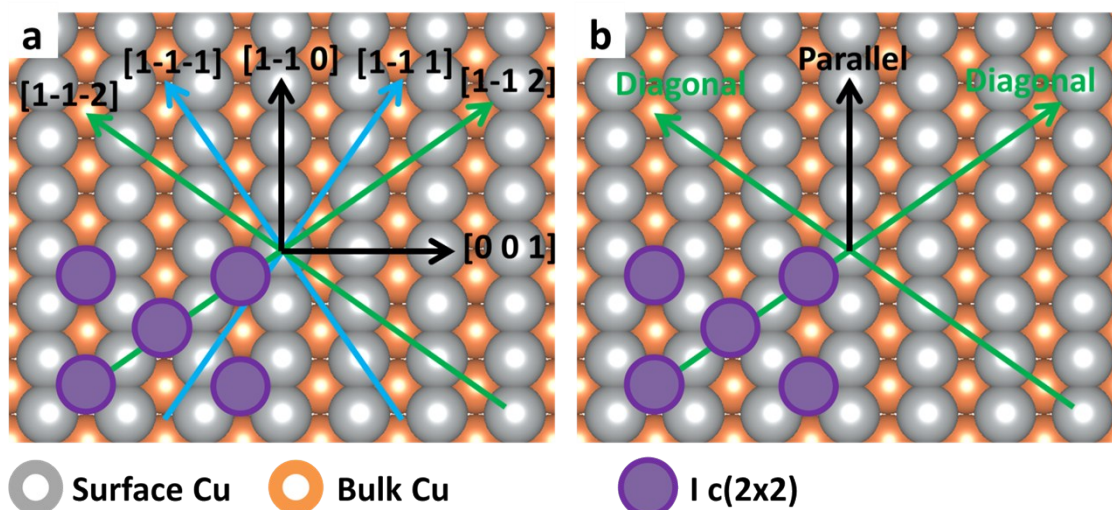


Figure S 2. Scheme of Cu(110) surface, with the most observed directions for the OM (a) and polymeric phase (b). Copper atoms are in grey and orange, iodine atoms in purple. All the OM structures are oriented along either the $[1-1\pm 1]$ or the $[1-1\pm 2]$, while the polymers are either along the $[1-1\pm 2]$ or $[1-10]$ direction.

4. Comparing dIB with other precursors

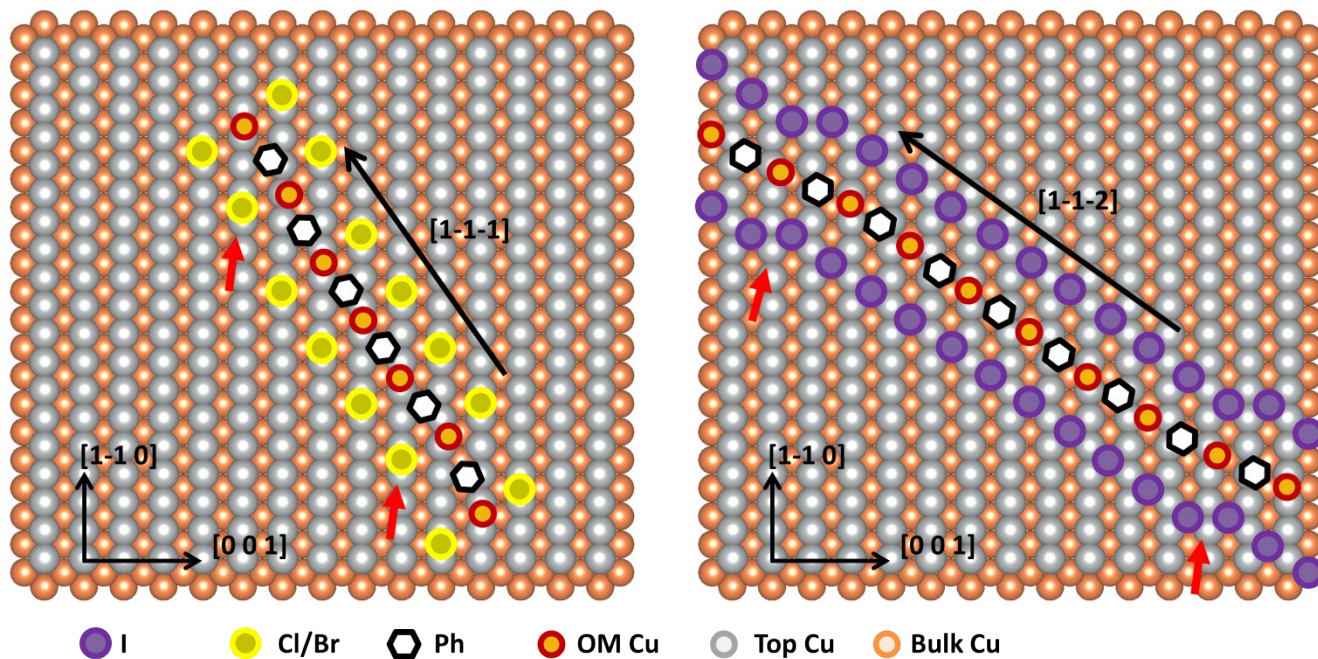


Figure S 3. Scheme of the long OM structures along $[1-1-1]$ direction (BCB, dCB, BIB) and $[1-1-2]$ direction (dIB) on Cu(110) surface. dIB follows a different behavior compared to the other precursors, as shown in Figure 4 of the manuscript. A clear difference is that iodine atoms adsorb at the hollow positions, while Br and Cl prefer short-bridge positions. Having halogens in different positions, forces the OM chains to self-assemble along different directions, with different structures

5. Short vs long OM chains for Cl-containing molecules

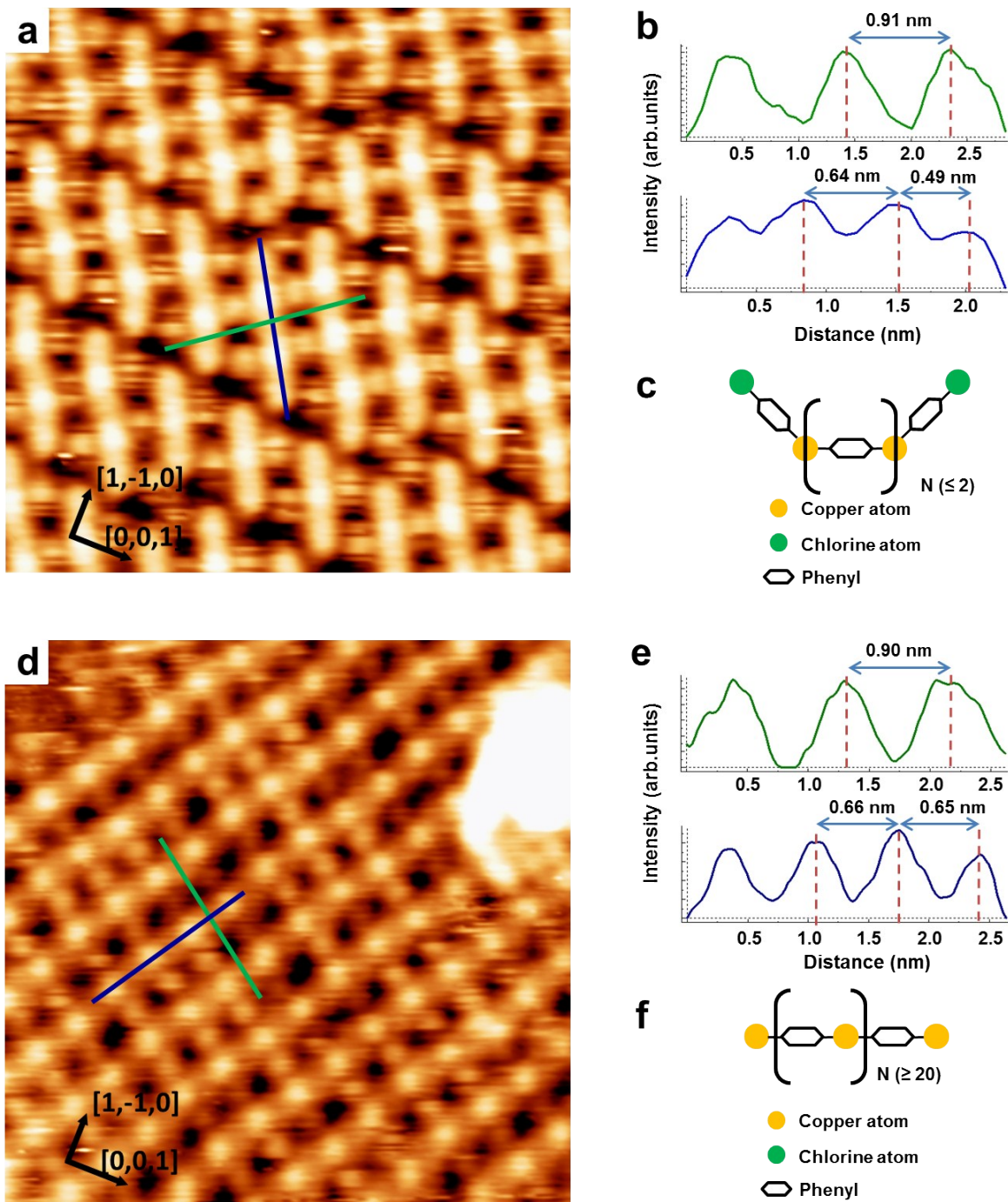


Figure S 4. STM images of OM chains formed by BCB on Cu(110), short chains are formed at RT, while long chains are formed after annealing at 150 °C. a) 8×8 nm² STM image of short OM chains along the $[1-1-1]$ direction ($V=-0.81$, $I= 1.46$ nA). b) Profiles intensities along the paths in (a). c) Side view of the hypothesized structure, with the terminal phenyls raised from the surface. d) 8×8 nm² STM image of long OM chains along the $[1-11]$ direction ($V=-0.87$, $I= 0.70$ nA). e) Profile intensities along the paths in (d). f) A model for the side view of the long OM structure in which the phenyls are Cu-terminated and flat.

6. Boundaries between OM chains and $c(2 \times 2)$ iodine domains for BIB

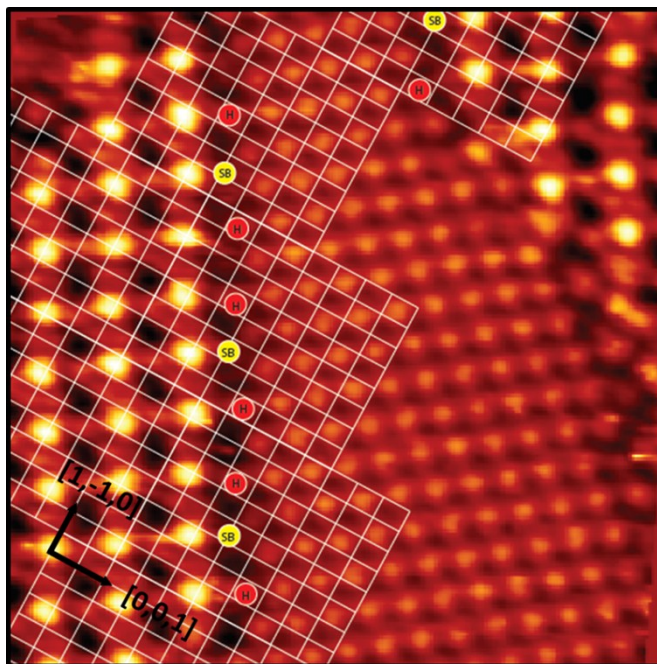


Figure S 5. $7 \times 7 \text{ nm}^2$ STM image of BIB on Cu(110) at RT, superimposed with the surface lattice. The halogens occupy two different lattice positions, short-bridge (SB) and hollow (H). We can therefore identify them as iodine (hollow assigned as H in red circle) and bromine (short-bridge assigned as SB in yellow circle).

7. NEXAFS results

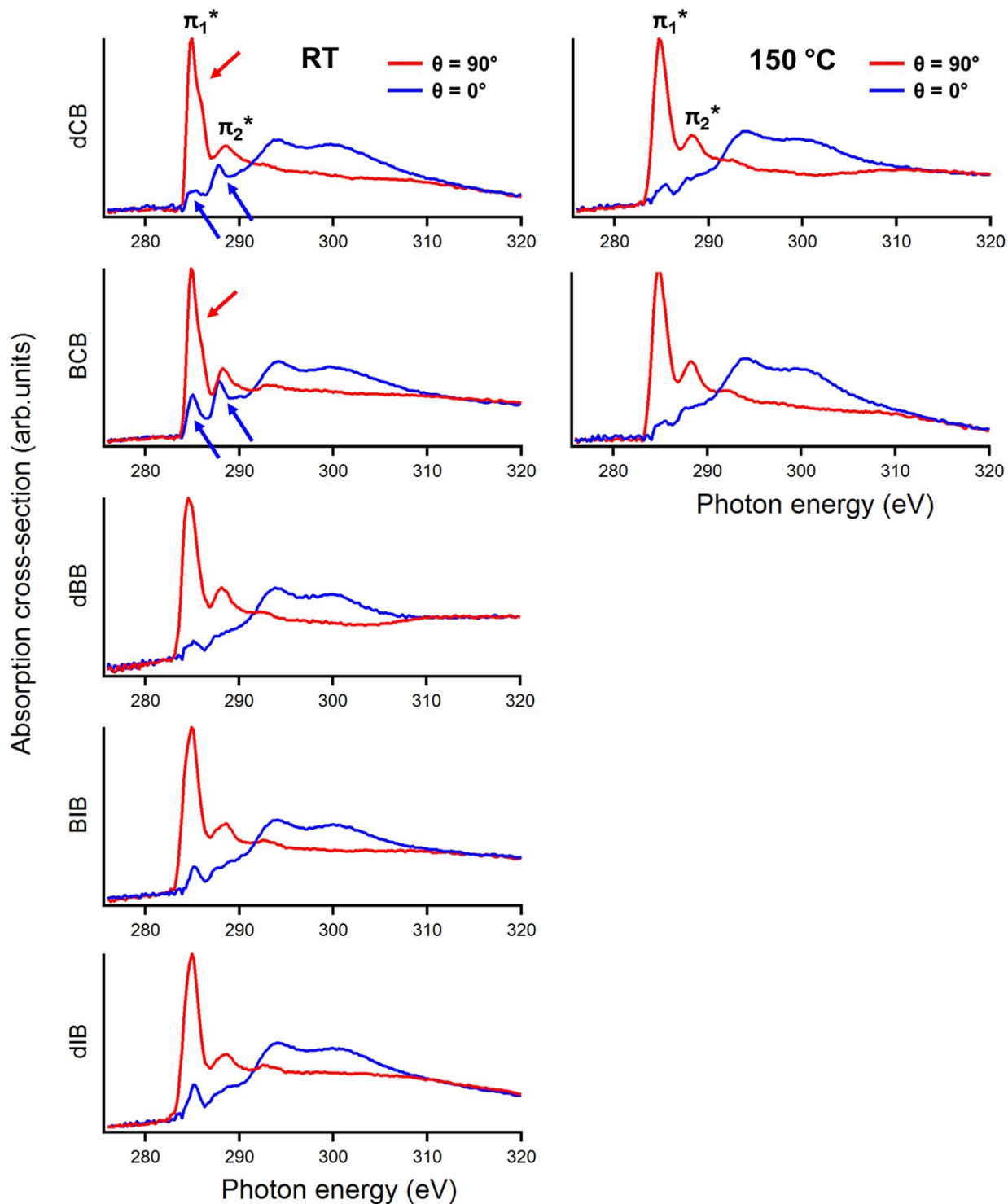


Figure S 6. Polarization-dependent C K-edge NEXAFS spectra for the five studied precursors at RT and for BCB and dCB at 150 °C. Two spectra are reported for each sample: $\theta = 90^\circ$ (blue, p-polarization) and $\theta = 0^\circ$ (red, s-polarization) with the incident radiation falling in the plane containing the sample normal and the [001] lattice direction. Red and blue arrows indicate important features observed only for chlorine-containing molecules at RT.

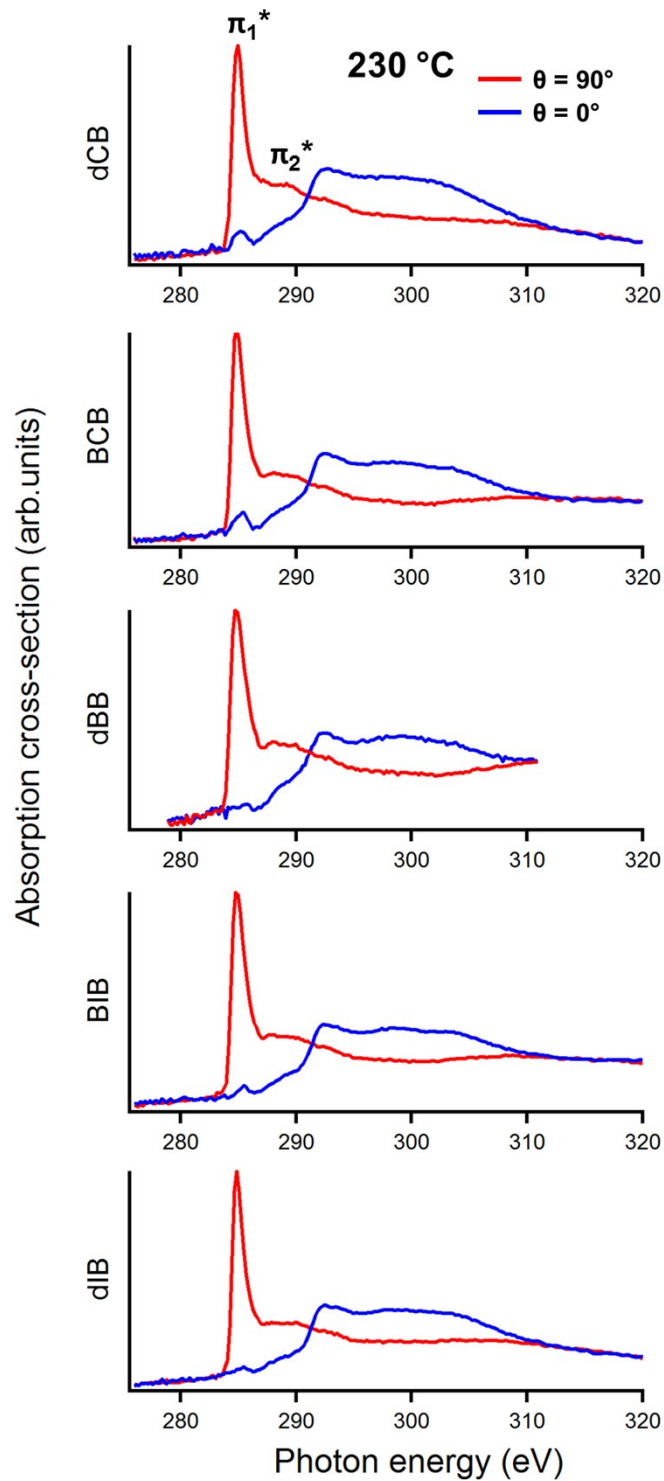


Figure S 7. Polarization-dependent C K-edge NEXAFS spectra for the five studied precursors at 230 °C; two spectra are reported for each sample: $\theta = 90^\circ$ (blue, p-polarization) and $\theta = 0^\circ$ (red, s-polarization) with the incident radiation falling in the plane containing the sample normal and the [001] lattice direction.

8. Simulated minimum energy path for halogens diffusion

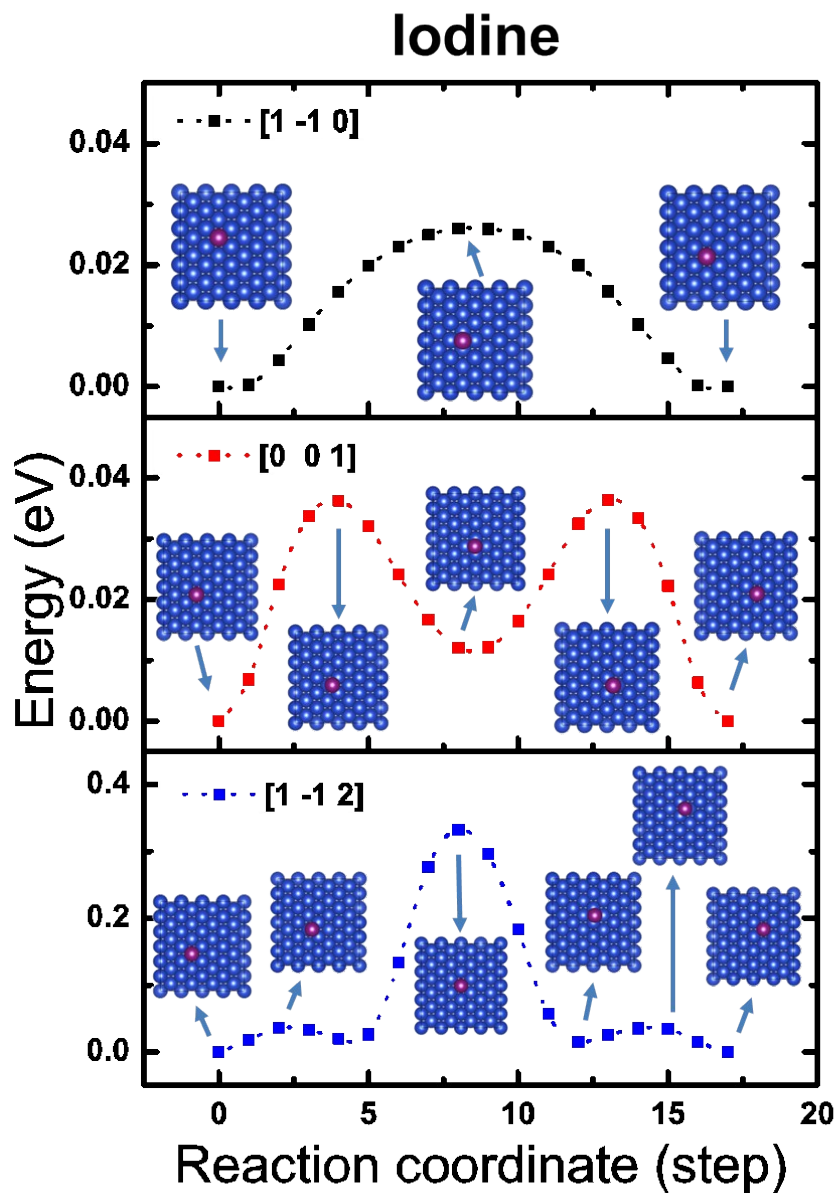


Figure S 8. DFT calculations of the minimum energy path for the diffusion of iodine along three directions of the Cu(110) surface, [1-10], [001] and [1-12]. The starting and ending adsorption positions for I are hollow sites. Some of the calculated structures along the path are displayed. The reaction coordinate is reported as the step number of the diffusion process. In every case, the last step corresponds to one unit cell movement along the studied direction.

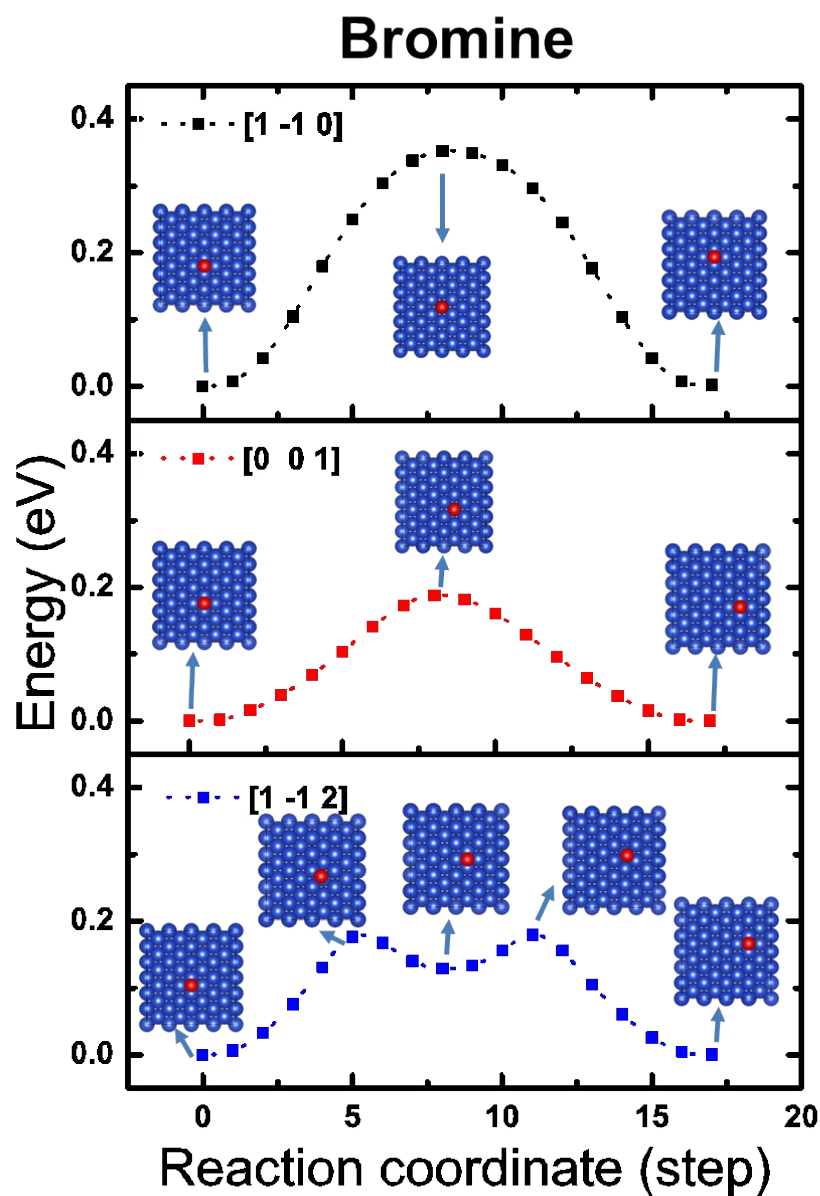


Figure S 9. DFT calculations of the minimum energy path for the diffusion of bromine along three directions of the Cu(110) surface, [1-10], [001] and [1-12]. The starting and ending adsorption positions for Br are short-bridge sites. Some of the calculated structures along the path are displayed. The reaction coordinate is reported as the step number of the diffusion process. In every case, the last step corresponds to one unit cell movement along the studied direction.

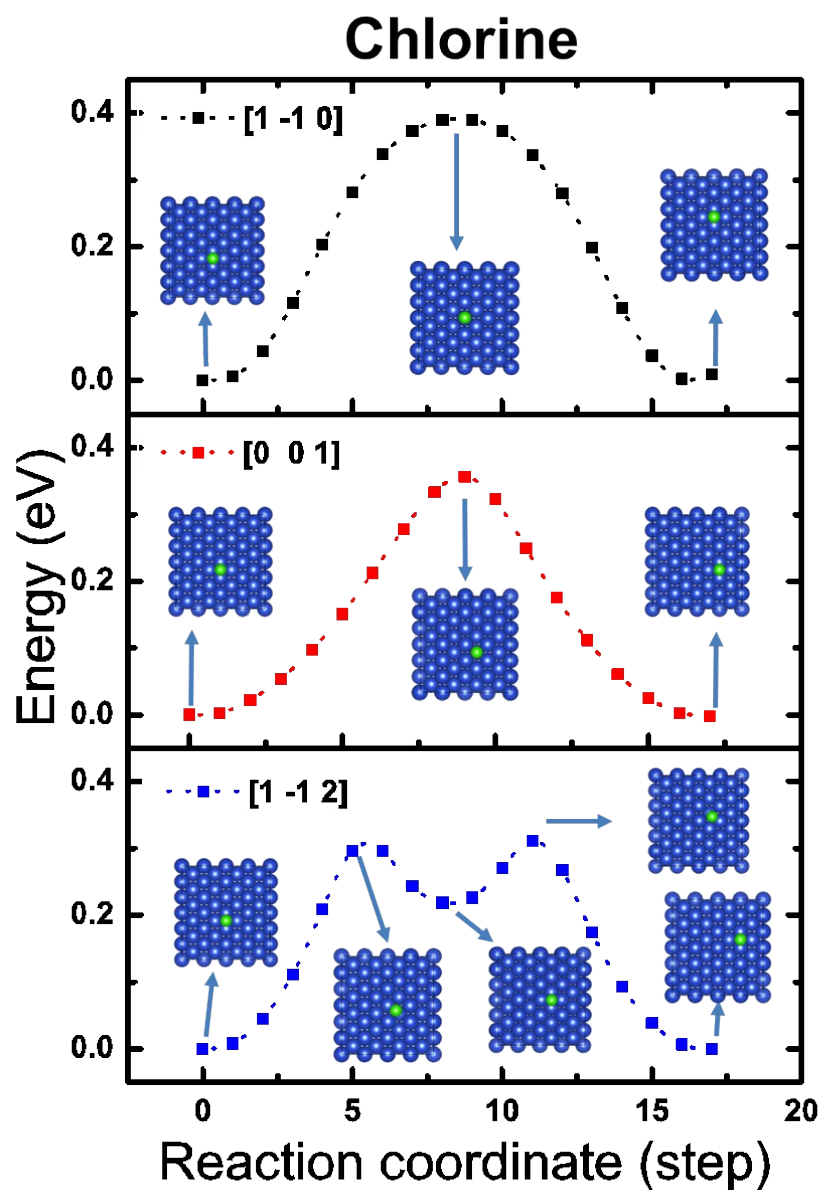
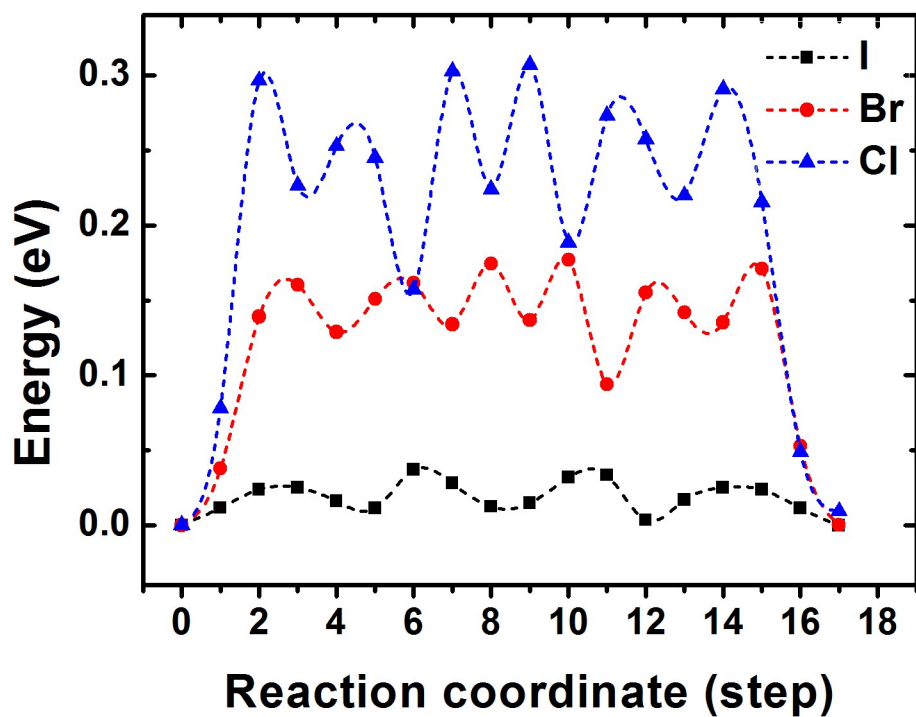


Figure S 10. DFT calculations of the minimum energy path for the diffusion of chlorine along three directions of the Cu(110) surface, [1-1 0], [001] and [1-1 2]. The starting and ending adsorption positions for Cl are short-bridge sites. Some of the calculated structures along the path are displayed. The reaction coordinate is reported as the step number of the diffusion process. In every case, the last step corresponds to one unit cell movement along the studied direction.



| | $E_d[001]$ (eV) | $E_d[1-10]$ (eV) | $E_d[1-12]$ (eV) | $E_d[1-11]$ (eV) |
|----|--------------------|---------------------|---------------------|---------------------|
| Cl | 0.36 (0.36) | 0.39 (0.40) | 0.31 (0.31) | 0.31 (0.31) |
| Br | 0.19 (0.18) | 0.35 (0.36) | 0.18 (0.18) | 0.17 (0.17) |
| I | 0.04 (0.04) | 0.03 (0.04) | 0.33 (0.36) | 0.04 (0.04) |

Figure S 11. top panel) DFT calculations of the minimum energy path for the diffusion of iodine, bromine and chlorine along the [1-11] direction. For Br and Cl, the equilibrium position is short-bridge, while for I is hollow. The last step corresponds to one unit cell movement along the [1-11] direction. Bottom panel) The summary of the diffusion energies (E_d) for I, Br and Cl along the studied directions using DFT and DFT-D3 (in parenthesis) calculation methods, described in the manuscript, Materials and methods section.